AEROFOIL AND WING PITCHING MOMENT COEFFICIENT AT ZERO ANGLE OF ATTACK DUE TO DEPLOYMENT OF TRAILING-EDGE PLAIN FLAPS AT LOW SPEEDS

1.   NOTATION AND UNITS

		SI	*British*
A	aspect ratio, $2s/\bar{c}$		
a_1	theoretical rate of change of lift coefficient with wing angle of attack	rad^{-1}	rad^{-1}
a_t	theoretical rate of change of lift coefficient for aerofoil with trailing-edge flap deflection, Equation (3.3)	deg^{-1}	deg^{-1}
C_L	lift coefficient; (lift)/qc for aerofoil, (lift)/qS for wing		
C_{L0}	lift coefficient at zero angle of attack for aerofoil, based on c		
ΔC_{L0t}	increment in lift coefficient at zero angle of attack due to deployment of trailing-edge plain flap on aerofoil, based on c		
C_m	pitching moment coefficient; (pitching moment)/qc^2 for aerofoil, (pitching moment)/$qS\bar{\bar{c}}$ for wing, referenced to $c/4$ for aerofoil and $\bar{\bar{c}}/4$ for wing, see Sketch 1.1		
$C_{m\alpha 0}$	pitching moment coefficient at zero angle of attack for aerofoil, based on c^2 and referenced to $c/4$		
$C_{mw\alpha 0}$	pitching moment coefficient at zero angle of attack for wing, based on $S\bar{\bar{c}}$ and referenced to $\bar{\bar{c}}/4$		
$\Delta C_{mt\alpha 0}$	increment in pitching moment coefficient at zero angle of attack due to deployment of trailing-edge plain flap on aerofoil, based on c^2 and referenced to $c/4$, see Equation (3.1)		
$\Delta C_{mtw\alpha 0}$	increment in pitching moment coefficient at zero angle of attack due to deployment of trailing-edge plain flap on wing, based on $S\bar{\bar{c}}$ and referenced to $\bar{\bar{c}}/4$, see Equation (3.6)		
c	basic (plain) aerofoil chord (*i.e.* chord with high-lift devices undeployed), see Sketch 1.2	m	ft
$\bar{c}$	wing geometric mean chord	m	ft
$\bar{\bar{c}}$	wing aerodynamic mean chord, see Item No. 76003 (Reference 32)	m	ft
c_r	wing root chord, see Sketch 1.2	m	ft

|			
c_t	chord of trailing-edge plain flap, see Sketch 1.2	m	ft
h_2	centre of incremental lift at zero angle of attack due to trailing-edge plain flap deflection on aerofoil section, expressed as fraction of chord, measured positive aft from aerofoil quarter-chord position, see Equation (3.5)		
h_{2T}	theoretical value of h_2, see Equation (3.4)		
J_p	efficiency factor for plain flap on aerofoil, required in Equation (3.2), see Figure 1		
J_{p0}	efficiency factor for plain flap on wing, required in Equation (3.7), see Figure 2		
K_f	flap-type correlation factor, see Equation (3.8)		
$K_{f\Lambda}$	flap-type correlation factor for wing sweep, see Equation (3.9)		
K	part-span factor; pitching moment coefficient increment due to part-span trailing-edge plain flaps extending symmetrically from wing centre-line divided by pitching moment coefficient increment due to full-span trailing-edge plain flaps at the same deflection angle and wing angle of attack, Figure 4		
K_i	value of K corresponding to $\eta = \eta_i$, required in Equation (3.6)		
K_o	value of K corresponding to $\eta = \eta_o$, required in Equation (3.6)		
K_Λ	part-span factor dependent on wing sweep effect, see Figure 5		
$K_{\Lambda i}$	value of K_Λ corresponding to $\eta = \eta_i$, required in Equation (3.6)		
$K_{\Lambda o}$	value of K_Λ corresponding to $\eta = \eta_o$, required in Equation (3.6)		
M	free-stream Mach number		
q	free-stream kinetic pressure	N/m^2	lbf/ft^2
R_c	aerofoil Reynolds number based on free-stream conditions and c		
$R_{\bar{\bar{c}}}$	wing Reynolds number based on free-stream conditions and $\bar{\bar{c}}$		
S	wing planform area, $2s\bar{c}$	m^2	ft^2
s	wing semi-span, see Sketch 1.1	m	ft
t	maximum thickness of aerofoil	m	ft
z_{um}	maximum upper surface ordinate of basic aerofoil, see Sketch 1.2	m	ft
β	compressibility parameter, $(1 - M^2)^{1/2}$		

$\delta_t{}^\circ$	deflection of trailing-edge flap, positive trailing edge down, see Sketch 1.2		deg	deg
η	spanwise distance from wing centre-line as fraction of semi-span			
η_i	value of η at inboard limit of flap, see Sketch 1.1			
η_o	value of η at outboard limit of flap, see Sketch 1.1			
Λ_0	wing leading-edge sweep angle, see Sketch 1.1		deg	deg
$\Lambda_{1/4}$	wing quarter-chord sweep angle, see Sketch 1.1		deg	deg
Λ_1	wing trailing-edge sweep angle, see Sketch 1.1		deg	deg
λ	wing taper ratio (tip chord/root chord)			
$\phi_t{}^\circ$	angle between aerofoil datum and tangent to upper surface at trailing edge, see Sketch 1.2		deg	deg

Subscripts

$\alpha 0$	denotes value at zero angle of attack
$(\ )_{expt}$	denotes experimental value
$(\ )_{pred}$	denotes predicted value
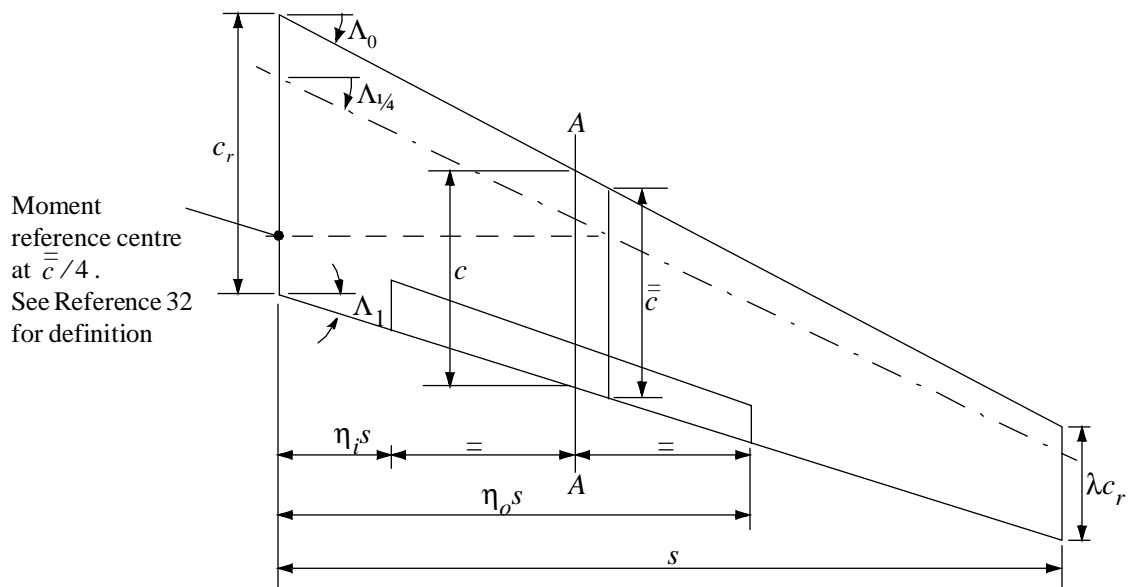
Sketch 1.1   Wing notation (flaps undeployed)
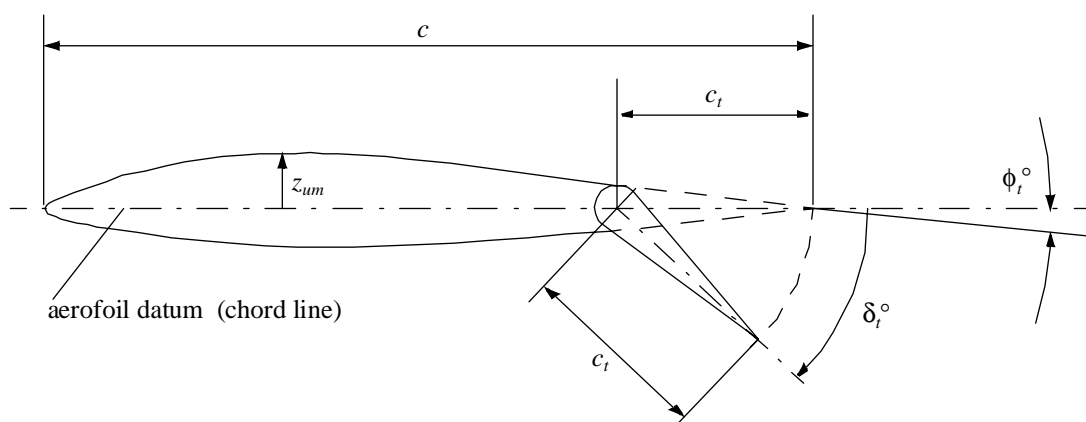
Sketch 1.2   Deployed plain flap notation (at Section AA)

2. INTRODUCTION

This Item provides a method to obtain the increment in pitching moment coefficient at zero angle of attack, due to deployment of trailing-edge plain flaps, either on an aerofoil or on a wing.

For aerofoils the method predicts the centre of lift position, h_2, due to plain flap deployment, based on the thin-aerofoil theory of Derivation 29 and modified to obtain correlation with the experimental data of Derivations 4 to 11, 22 and 23. This is combined with the increment in aerofoil lift coefficient calculated from Item No. 94028 (Derivation 2) to estimate the pitching moment coefficient increment.

For wings with full-span trailing-edge plain flaps, factors, dependent on planform geometry, are applied to the pitching moment coefficient increment on a section that is representative of the wing, to allow for three-dimensional effects. Derivations 30 and 31 were used as the basis for these factors, with some adjustment to the simple theoretical assumptions. The method of Item No. 97011 (Derivation 3) is used (instead of Item No. 94028) to predict the increment in section lift to obtain the section pitching moment increment. For wings with part-span trailing-edge flaps, additional factors are introduced that are dependent on taper ratio, aspect ratio, sweep and spanwise extent of the flap.

Section 3 describes the prediction method and Section 4 discusses Mach number and Reynolds number effects. The accuracy and applicability of the method are addressed in Section 5. The Derivation and References are given in Section 6. Section 7 illustrates worked examples for an aerofoil and a wing.

3. PREDICTION METHOD

The method for aerofoils requires the use of Item No. 94028, to determine the lift increment characteristics of the aerofoil/flap combination from which to derive the pitching moment coefficient increment.

However, for wings the method requires the use of Item No. 97011 to determine the lift increment characteristics of the representative section/flap combination from which to derive the section pitching moment coefficient increment. The *streamwise* section and flap geometries and angles at the mid-span of the flap panel are taken to be representative of the wing/flap system, see Sketches 1.1 and 1.2. By this means, the effects of spanwise variation are averaged out. Empirical corrections allow for the effects of wing planform geometry and the spanwise extent of the flaps.

3.1 Aerofoil Pitching Moment Coefficient Increment $\Delta C_{mt\alpha0}$

The increment in the pitching moment coefficient at zero angle of attack for deployment of a plain flap on an aerofoil is obtained as the product

$$\Delta C_{mt\alpha0} = -\Delta C_{L0t}h_2 . \tag{3.1}$$

Here, ΔC_{L0t} is the increment in lift coefficient at zero angle of attack due to deployment of a plain flap on an aerofoil and is evaluated as

$$\Delta C_{L0t} = J_p a_t \delta_t^\circ , \tag{3.2}$$

where J_p is an empirical efficiency factor taken from Item No. 94028, and is given in Figure 1 as a function of the angle $(\delta_t^\circ + \phi_t^\circ)$, see Sketch 1.2, and a_t is the theoretical rate of change of lift coefficient with

respect to the deflection angle $\delta_t{}^\circ$, positive trailing edge down, at constant angle of attack, given by thin-plate theory as

$$a_t = (\pi/90)\left\{\pi - \cos^{-1}(2c_t/c - 1) + [1 - (2c_t/c - 1)^2]^{1/2}\right\}. \qquad (3.3)$$

Values of a_t have been evaluated and the results are presented in Figure 2a.

The centre of the lift increment at zero angle of attack, h_2, expressed as a fraction of the chord and measured positive aft from the quarter-chord point, is derived empirically from its theoretical value in Derivation 29 for a hinged plate on a thin aerofoil

$$h_{2T} = 0.25[1 - (2c_t/c - 1)^2]^{1/2}[1 - (2c_t/c - 1)] \Big/ \left\{\pi - \cos^{-1}(2c_t/c - 1) + [1 - (2c_t/c - 1)^2]^{1/2}\right\}. \qquad (3.4)$$

Values of h_{2T} have been evaluated and are given in Figure 2b.

An incremental adjustment to obtain correlation with experimental data gives

$$h_2 = h_{2T} + 0.012(44 - \delta_t{}^\circ)\, z_{um}/c + 0.011(c_t/c)^3\delta_t{}^\circ, \qquad (3.5)$$

where

c_t/c is the ratio of the flap chord to the aerofoil chord,

$\delta_t{}^\circ$ is the flap deflection angle, in degrees,

and

z_{um}/c is the ratio of the maximum upper-surface ordinate to the aerofoil chord as shown in Sketch 1.2.

3.2   Wing Pitching Moment Coefficient Increment $\Delta C_{mtw\alpha 0}$

For a wing at zero angle of attack the increment in pitching moment coefficient due to plain flap deployment is correlated to be

$$\Delta C_{mtw\alpha 0} = -K_f(K_o - K_i)\Delta C_{L0t}h_2 + K_{f\Lambda}(K_{\Lambda o} - K_{\Lambda i})(A/2)\Delta C_{L0t}\tan\Lambda_{1/4}, \qquad (3.6)$$

where A is the aspect ratio and ΔC_{L0t} is now calculated for the representative section of the wing, taken at flap mid-span and, instead of Equation (3.2),

$$\Delta C_{L0t} = J_{p0}a_t\delta_t{}^\circ, \qquad (3.7)$$

where J_{p0} is an empirical efficiency factor for a plain flap on the representative section, taken from Item No. 97011 and given in Figure 3.

The part-span factors K_i and K_o are obtained from Figure 4 as functions of taper ratio and the inboard and outboard limits of the trailing-edge plain flap, η_i and η_o respectively.

The flap type correlation factors for plain flaps have been derived from the data of Derivations 12 to 17 and 20 to be

$$K_f = (a_1/2\pi)^{0.46} \tag{3.8}$$

and $\quad\quad\quad K_{f\Lambda} = \cos\Lambda_{1/4}, \tag{3.9}$

where a_1 is the wing lift slope obtained from Item No. 70011 (Derivation 1).

The part-span wing sweep factors $K_{\Lambda i}$ and $K_{\Lambda o}$ are obtained for plain flaps from Figure 5 as functions of taper ratio and the inboard and outboard limits of the trailing-edge plain flap, η_i and η_o respectively.

Note that for all cases with a full-span plain flap or an unswept quarter-chord line the second term in Equation (3.6) has a value of zero.

The data for K_Λ were obtained from Derivation 30 in the simplified form

$$K_\Lambda = \frac{\eta(1-\eta)[(1+2\lambda) - \eta(1-\lambda^2)]}{4(1+\lambda+\lambda^2)}, \tag{3.10}$$

which is equivalent to Figure 5.

4. EFFECTS OF MACH NUMBER AND REYNOLDS NUMBER

4.1 Mach Number Effects

High local Mach numbers will occur at low free-stream Mach number as a result of high angle deployment of trailing-edge plain flaps. Significant Mach number effects will occur at free-stream Mach numbers greater than about 0.2, at large values of $(\delta_t{}^\circ + \phi_t{}^\circ)$, and at progressively smaller values as Mach number is increased. None of the data considered for this Item was for a Mach number greater than 0.27.

4.2 Reynolds Number Effects

For the data used in the derivation of this Item no effect of Reynolds number on $\Delta C_{mt\alpha0}$ or $\Delta C_{mtw\alpha0}$ was found over the ranges of Reynolds number shown in Tables 5.1 and 5.2.

5. APPLICABILITY AND ACCURACY

5.1 Applicability

5.1.1 Aerofoils

The method given in this Item for estimating the position of the centre of the lift increment and of the increment in pitching moment coefficient at zero angle of attack, due to deployment of a trailing-edge plain flap, applies only to aerofoils without the deployment of a leading-edge device and with no chord extension.

Table 5.1 summarises the parameter ranges covered by the experimental data, obtained from Derivations 4 to 11, 22, 23 and 25, from which Equation (3.5) was derived to obtain correlation.

TABLE 5.1 Parameter ranges for test data for trailing-edge plain flaps on aerofoils used in the method of Section 3.1

Parameter	Range
t/c	0.06 to 0.16
z_{um}/c	0.03 to 0.093
c_t/c	0.1 to 0.5
δ_t°	5º to 75º
$\delta_t^\circ + \phi_t^\circ$	12º to 84º
$R_c \times 10^{-6}$	1.0 to 9.0
M	0.11 to 0.17

5.1.2 Wings

The method given in this Item for estimating the increment in pitching moment coefficient at zero angle of attack, due to deployment of a trailing-edge plain flap on a wing, has been shown to be applicable to straight-tapered wings covering a wide range of planform parameters. Table 5.2 summarises the parameter ranges covered by the experimental data that were obtained from Derivations 12 to 21, 24 and 26 to 28 and used in the development of the method. Note that the method should apply to the full range of chord ratios and flap angles in Table 5.1.

For a wing where c_t/c is not constant, the flap should be divided into several spanwise portions, calculation made separately for each, using the mid-span geometries, and the results summed to provide a total value of $\Delta C_{mtw\alpha 0}$. The number of portions required will depend on how rapidly the ratio c_t/c varies across the span.

No wings with cranked leading or trailing edges or curved tips were included in the analysis. It is suggested that for such wings the planform parameters λ and $\Lambda_{1/4}$ be calculated for the equivalent straight-tapered planform as defined in Item No. 76003 (Reference 32). Care should be taken with the definition of c_t/c and the user of the final result should be aware of the non-validated use of the method for such wings.

TABLE 5.2 Parameters ranges for test data for trailing-edge plan flaps on wings used in the method of Section 3.2

| Parameter	Range
A	2.0 to 9.0
$A \tan \Lambda_0$	0 to 6.9
$A \tan \Lambda_{1/2}$	-0.4 to 5.7
Λ_0	0 to 63°
Λ_1	$-11°$ to 58°
λ	0.25 to 1.0
c_t/c	0.19 to 0.30
$\delta_t°$	2° to 60°
$\delta_t° + \phi_t°$	6° to 72°
η_i	0 to 0.73
η_o	0.32 to 1.0
$R_c \times 10^{-6}$	0.9 to 4.5
M	$\leq$ 0.27

5.2 Accuracy

5.2.1 Aerofoils

Sketch 5.1 shows the comparison between predicted and experimental values of the centre of the lift increment, h_2, due to deployment of trailing-edge plain flaps on an aerofoil, for data from Derivations 4 to 11, 22, 23 and 25, and 92% are correlated to within ± 0.02. Sketch 5.2 shows the corresponding comparison between predicted and experimental values of pitching moment coefficient increments, where 95% of the data are correlated to within ± 0.04.

5.2.2 Wings

The comparison between predicted and experimental values of the pitching moment coefficient increment, $\Delta C_{mtw\alpha 0}$, due to deployment of both full-span and part-span trailing-edge plain flaps is shown on Sketch 5.3 for unswept wings and on Sketch 5.4 for swept wings, for data from Derivations 12 to 21, 24 and 26 to 28. In the two sketches 93% of the data are correlated to within ± 0.02 and the rms error is 0.010.
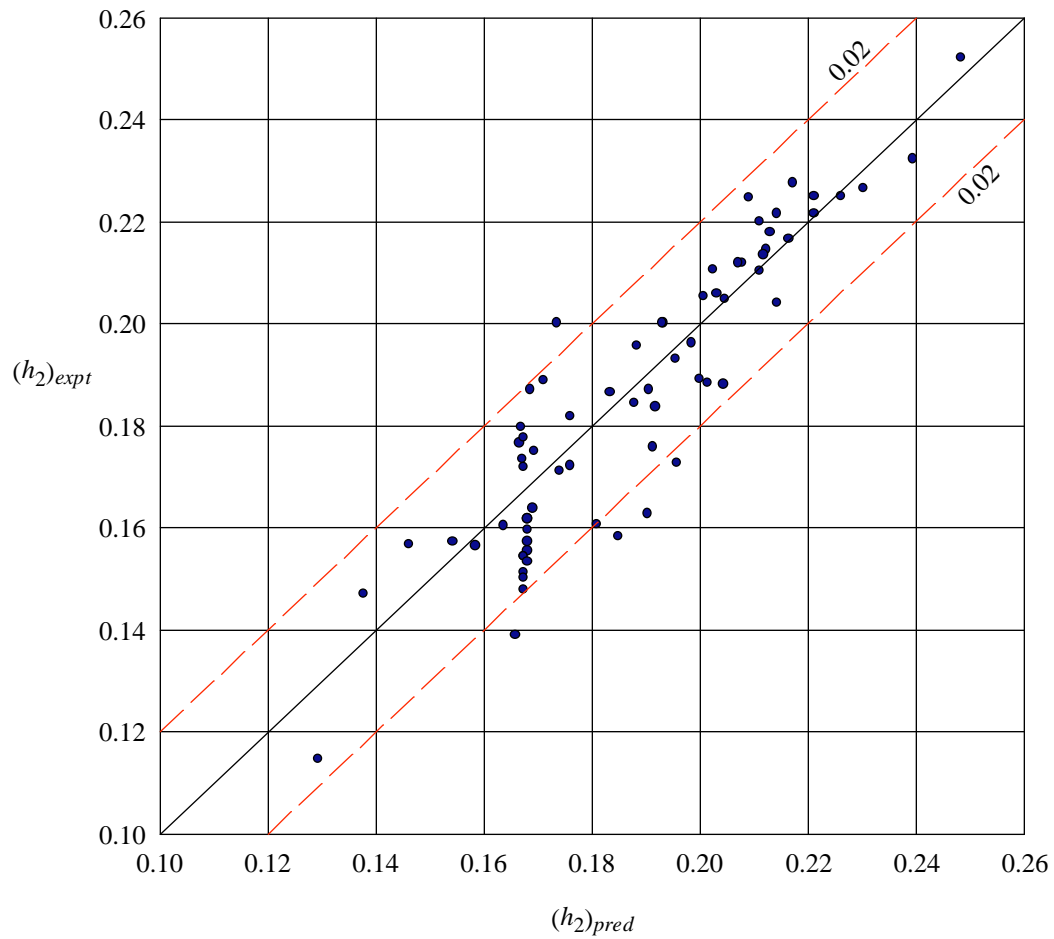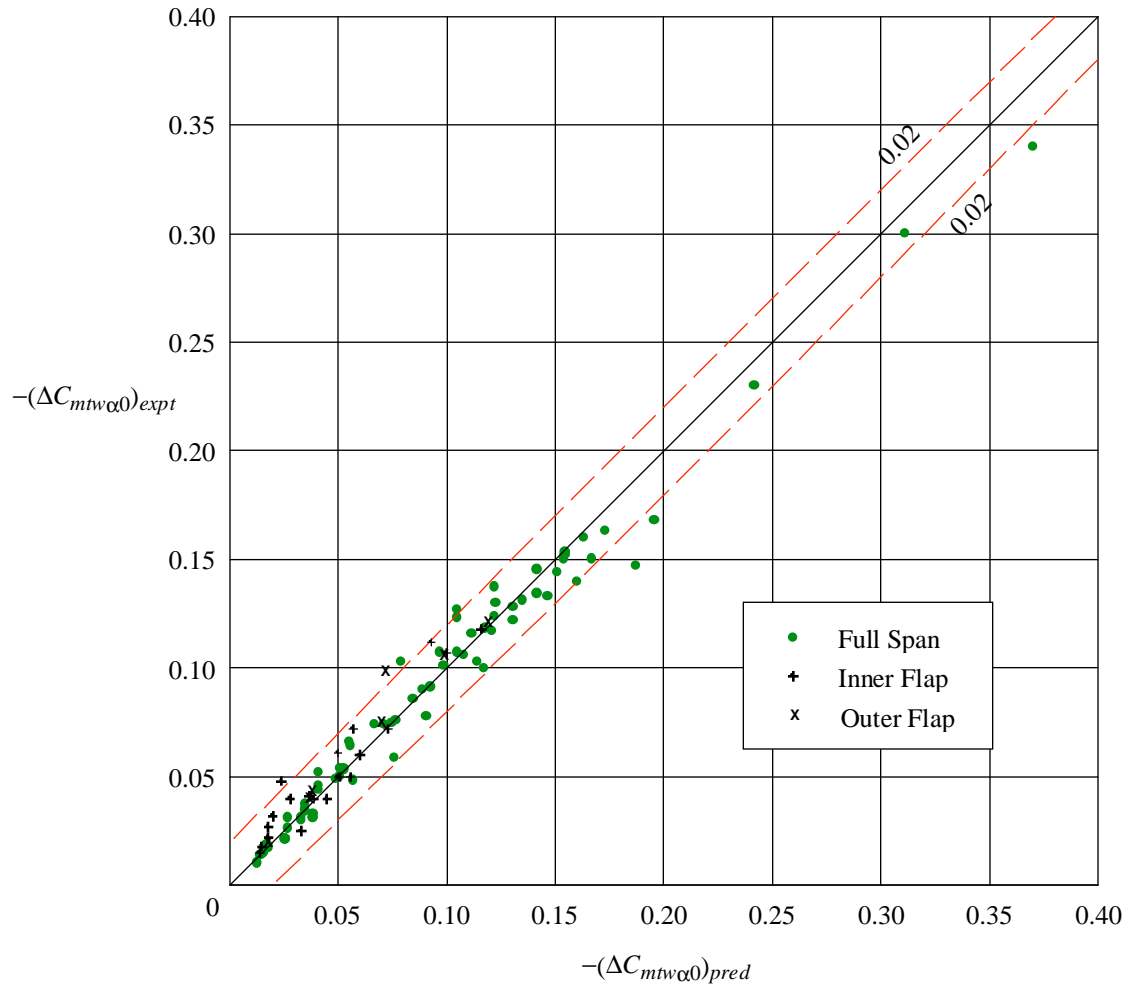
Sketch 5.1   Comparison of predicted and experimental values of h_2
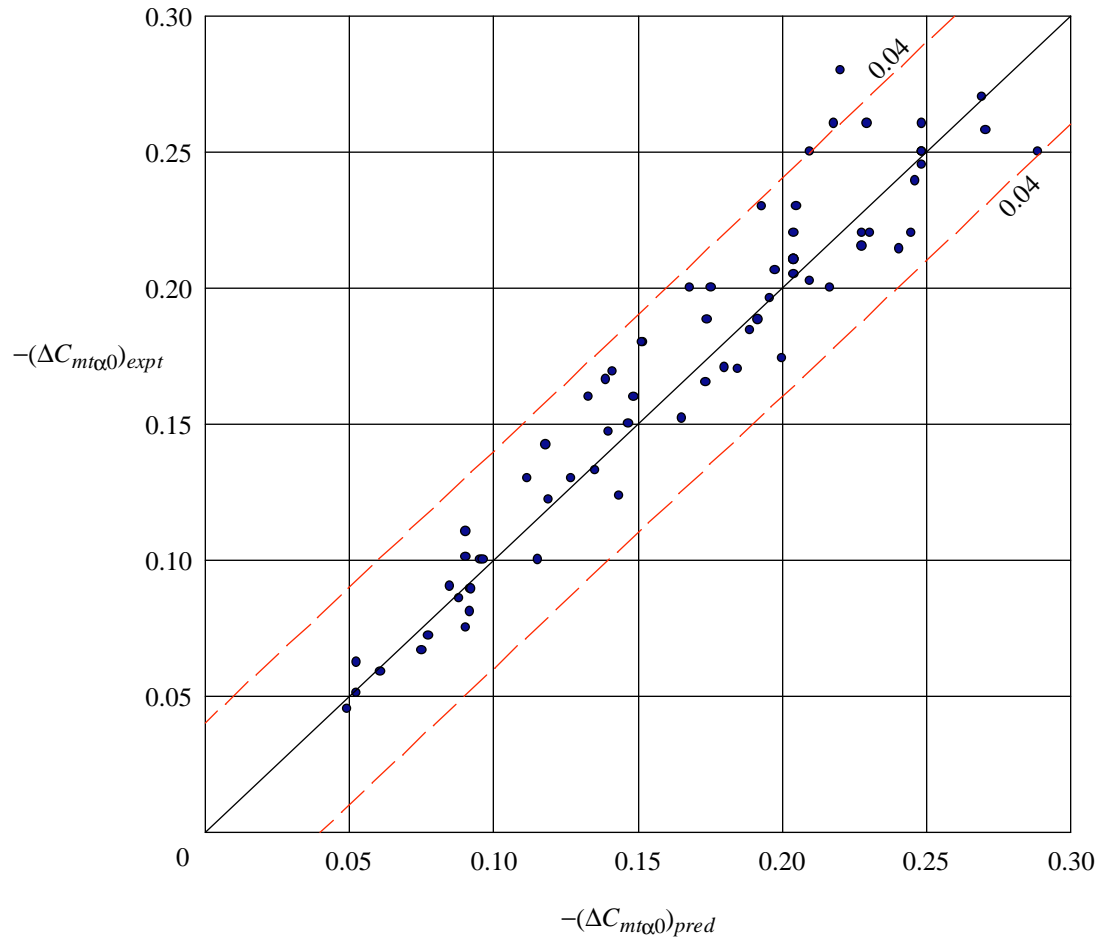
Sketch 5.2   Comparison of predicted and experimental values of $\Delta C_{mt\alpha 0}$ for deployment of plain flaps on aerofoils
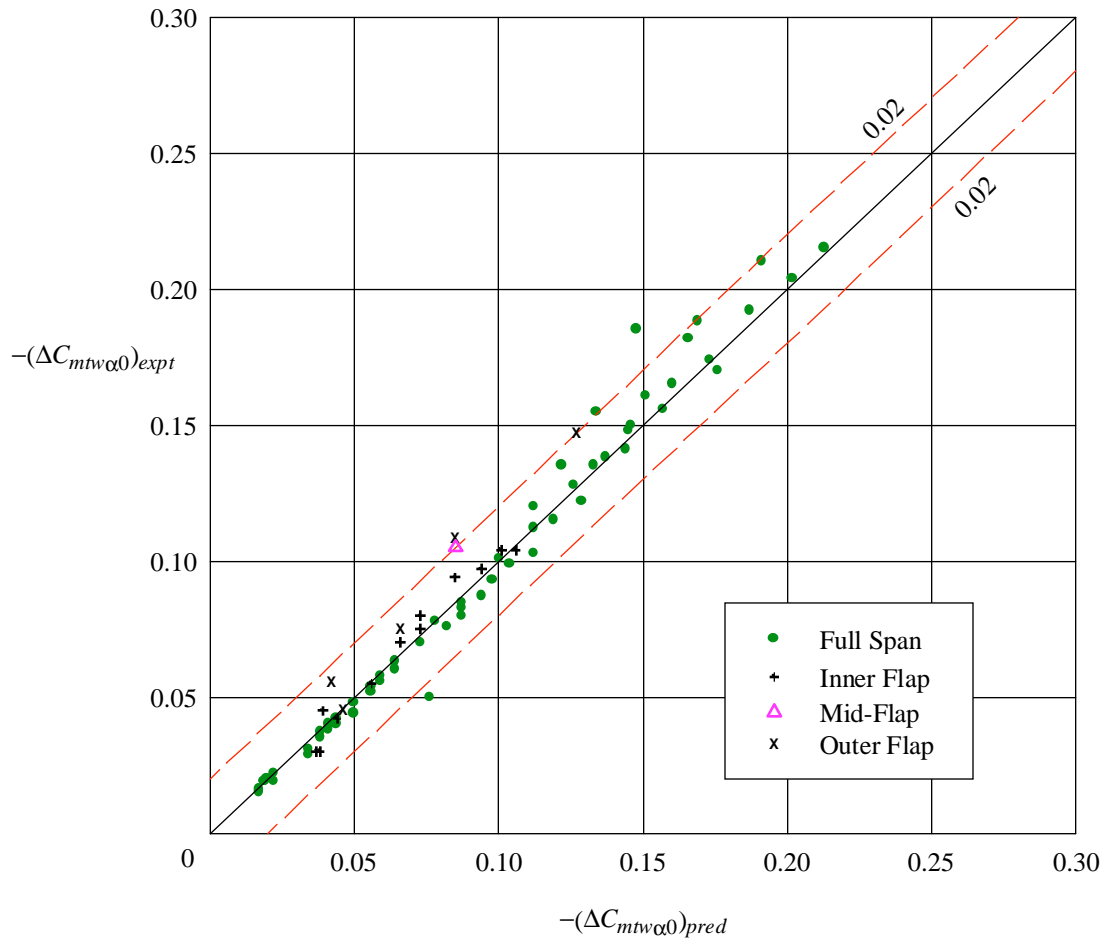
Sketch 5.3   Comparison of predicted and experimental values of $\Delta C_{mtw\alpha 0}$ for deployment of plain flaps on unswept wings

Sketch 5.4 Comparison of predicted and experimental values of $\Delta C_{mtw\alpha 0}$ for deployment of plain flaps on swept wings

6. DERIVATION AND REFERENCES

6.1 Derivation

The Derivation lists selected sources of information that have been used in the preparation of this Item.

6.1.1 ESDU Data Items

1.	ESDU	Lift-curve slope and aerodynamic centre position of wings in inviscid subsonic flow. ESDU International, Item No. 70011, 1970. ESDUpac A7011.
2.	ESDU	Increments in aerofoil lift coefficient at zero angle of attack and in maximum lift coefficient due to deployment of a plain trailing-edge flap, with or without a leading-edge high-lift device, at low speeds. ESDU International, Item No. 94028, 1994.
3.	ESDU	Wing lift coefficient increment at zero angle of attack due to deployment of plain trailing-edge flaps at low speeds. ESDU International, Item No. 97011, 1997.

6.1.2 Wind-tunnel test reports

4.	WENZINGER, C.J. DELANO, J.B.	Pressure distribution over an NACA 23012 aerofoil with a slotted and plain flap. NACA Report 633, 1938.
5.	WENZINGER, C.J. HARRIS, T.A.	Wind-tunnel investigation of an NACA 23012 aerofoil with various arrangements of slotted flaps. NACA Report 664, 1938.
6.	WENZINGER, C.J. GAUVAIN, W.E.	Wind-tunnel investigation of an NACA aerofoil with a slotted flap and three types of auxiliary flap. NACA Report 679, 1939.
7.	STREET, W.G. AMES, M.B.	Pressure distribution investigation of an NACA 0009 aerofoil with a 50% chord plain flap and three tabs. NACA tech. Note 734, 1939.
8.	AMES, M.B SEARS, R.I.	Pressure distribution investigation of an NACA 0009 aerofoil with a 30% chord plain flap and three tabs. NACA tech. Note 759, 1940.
9.	UNDERWOOD, W.J. BRASLOW, A.L. CAHILL, J.F.	Two-dimensional wind-tunnel investigation of 0.20 aerofoil chord plain ailerons of different contour on an NACA 65_1210 aerofoil section. NACA WR L-151, 1945.
10.	STEVENSON, D.B. BYRNE, Y.W.	High speed wind-tunnel tests of an NACA 16-009 aerofoil having a 32.9% chord flap with an overhang 20.1% of the flap chord. NACA tech. Note 1406, 1947.
11.	STEVENSON, D.B. ADLER, A.A.	High speed wind-tunnel tests of an NACA 0009-64 airfoil having a 33.4% chord flap with an overhang 20.1% of the flap chord. NACA tech. Note 1417, 1947.

12.	DODS, J.B.	Wind-tunnel investigation of horizontal tails. I – unswept and 35° swept-back plan forms of aspect ratio 3. NACA RM A7K24 (TIL 1793), 1948.
13.	DODS, J.B.	Wind-tunnel investigation of horizontal tails. II – unswept and 35° swept-back plan forms of aspect ratio 4.5. NACA RM A8B11 (TIL 1831), 1948.
14.	DODS, J.B.	Wind-tunnel investigation of horizontal tails. III – unswept and 35° swept-back plan forms of aspect ratio 6. NACA RM A8H30 (TIL 2012), 1948.
15.	DODS, J.B.	Wind-tunnel investigation of horizontal tails. IV – unswept plan form of aspect ratio 2 and a two-dimensional model. NACA A8J21 (TIL 2028), 1948.
16.	HOPKINS, E.J.	Aerodynamic study of a wing-fuselage combination employing a wing swept back 63°. Effects of split flaps, elevons, and leading-edge devices at low speed. NACA RM A9C21 (TIL 2127), 1949.
17.	DODS, J.B.	Wind-tunnel investigation of horizontal tails. V – 45° swept-back plan form of aspect ratio 2. NACA RM A9D05 (TIL 2114), 1949.
18.	JOHNSON, H.S. HAGERMAN, J.R.	Wind-tunnel investigation at low speed of an unswept untapered semi-span wing of aspect ratio 3.13 equipped with various 25-percent-chord plain flaps. NACA tech. Note 2080, 1950.
19.	PASAMANICK, J. SELLERS, T.B.	Low speed investigation of leading-edge and trailing-edge flaps on a 47.5° swept-back wing of aspect ratio 3.4 at a Reynolds number of 4.4×10^6. NACA RM L50E02 (TIL 2404), 1950.
20.	KOLBE, D.C. BANDETTINI, A.	Investigation in the Ames 12-foot pressure wind-tunnel of a model horizontal tail of aspect ratio 3 and taper ratio 0.5 having the quarter-chord line swept back 45°. NACA RM A51D02 (TIL 2780), 1951.
21.	LICHTENSTEIN, J.H. WILLIAMS, J.L.	Effect of high-lift devices on the static-lateral-stability derivatives of a 45° swept-back wing of aspect ratio 4.0 and taper ratio 0.6 in combination with a body. NACA tech. Note 2819, 1952.
22.	CAHILL, J.F.	Aerodynamic forces and loadings on symmetrical circular arc airfoils with plain leading-edge and plain trailing-edge flaps. NACA Report 1146, 1953.
23.	GAINBUCCI, B.J.	Section characteristics of the NACA 0006 airfoil with leading-edge and trailing-edge flaps. NACA tech. Note 3797, 1956.
24.	JAMES, H.A. HUNTON, L.W.	Estimation of incremental pitching moments due to trailing-edge flaps on swept and triangular wings. NACA tech. Note 4040, 1957.

25.	ABBOTT, I.H. VON DOENHOFF, A.E.	*Theory of Wing Sections.* Dover Publications, New York, 1959.
26.	HEBERT, J.	STOL tactical aircraft investigation. Volume IV. Wind-tunnel data analysis. AFFDL TR 73-21. General Dynamics Corporation (Convair Aerospace Division) AD–767 363, 1973.
27.	MORGAN, H.L. PAULSON, J.W.	Aerodynamic charactics of wing-body configuration with two advanced general aviation airfoil sections and simple flap systems. NASA tech. Note D-8524, 1977
28.	RAE	Unpublished data, 1978.

6.1.3 Theory

29.	GLAUERT, H.	Theoretical relationships for an aerofoil with hinged flap. ARC R&M 1095, 1927.
30.	DENT, M.M CURTIS, M.F.	A method of estimating the effect of flaps on pitching moment and lift on tailless aircraft. RAE Report No. Aero 1861, 1943.
31.	YOUNG, A.D.	The aerodynamic characteristics of flaps. ARC R&M 2622, (RAE Report No. Aero 2185), 1947.

6.2 References

The References list selected sources of information supplementary to that given in this Item.

32.	ESDU	Geometrical properties of cranked and straight tapered wing planforms. ESDU International, Item No. 76003, 1976.

7. EXAMPLES

7.1 Example 1: Pitching Moment Increment due to a Plain Trailing-edge Flap on an Aerofoil
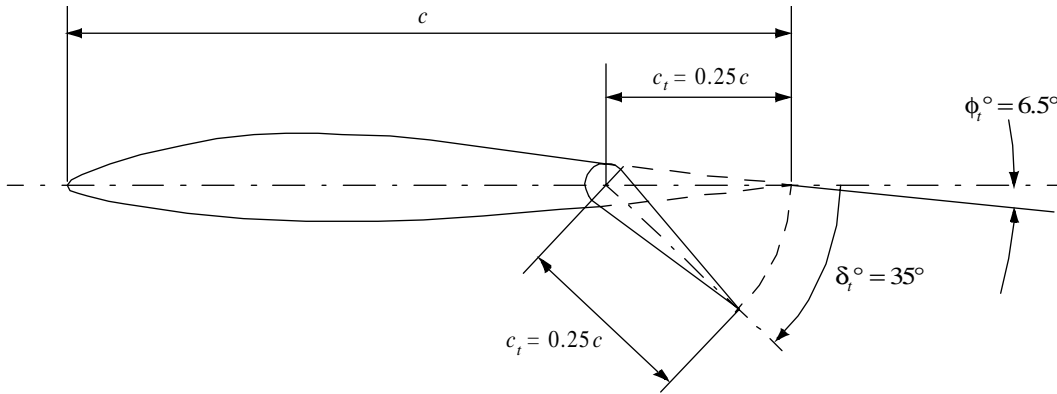
Estimate the increment in pitching moment coefficient at zero angle of attack due to the deployment of a plain trailing-edge flap installed on a NACA 63_1-212 section .

The required geometrical parameters are

$$c_t/c = 0.25 \quad \text{and} \quad \delta_t° = 35°,$$
$$z_{um}/c = 0.07 \quad \text{and} \quad \phi_t° = 6.5°.$$

The flow conditions are $M = 0.2$ and $R_c = 4.5 \times 10^6$, both of which are within the ranges of Table 5.1

Sketch 7.1   Flap Geometry

(1)   Determine ΔC_{L0t}

From Equation (3.3)

$$a_t = (\pi/90) \left\{ \pi - \cos^{-1}(2c_t/c - 1) + [1 - (2c_t/c - 1)^2]^{1/2} \right\}$$

$$= (3.142/90) \left\{ 3.142 - \cos^{-1}(2 \times 0.25 - 1) + [1 - (2 \times 0.25 - 1)^2]^{1/2} \right\}$$

$$= 0.0668 \text{ deg}^{-1}.$$

From Figure 1, with $\delta_t° = 35°$ and $\phi_t° = 6.5°$ so that $\delta_t° + \phi_t° = 41.5°$,

$$J_p = 0.463.$$

From Equation (3.2)

$$\Delta C_{L0t} = J_p a_t \delta_t°$$
$$= 0.463 \times 0.0668 \times 35$$
$$= 1.082.$$

(2)   Determine h_2

From Equation (3.4)

$$h_{2T} = 0.25[1-(2c_t/c-1)^2]^{1/2}[1-(2c_t/c-1)]\Big/\Big\{\pi-\cos^{-1}(2c_t/c-1)+[1-(2c_t/c-1)^2]^{1/2}\Big\}$$

$$= 0.25[1-(2\times0.25-1)^2]^{1/2}[1-(2\times0.25-1)]\Big/\Big\{\pi-\cos^{-1}(2\times0.25-1)+[1-(2\times0.25-1)^2]^{1/2}\Big\}$$

$$= 0.1697$$

From Equation (3.5)

$$h_2 = h_{2T} + 0.012(44-\delta_t^\circ)\,z_{um}/c + 0.011(c_t/c)^3\delta_t^\circ$$

$$= 0.1697 + 0.012(44-35)\times0.07 + 0.011\times(0.25)^3\times35$$

$$= 0.1833\,.$$

(3)   Determine $\Delta C_{mt\alpha0}$

From Equation (3.1)

$$\Delta C_{mt\alpha0} = -\Delta C_{L0t}h_2$$

$$= -1.082\times0.1833$$

$$= -0.1983$$

$$\approx -\mathbf{0.198}\,.$$

**7.2   Example 2: Pitching Moment Increment due to a Plain Trailing-edge Flap on a Wing**

Estimate the increment in pitching moment coefficient at zero angle of attack for a Reynolds number $R_{\bar{c}} = 4.5\times10^6$ and a free-stream Mach number $M = 0.2$ for the wing with a part-span trailing-edge plain flap shown in Sketch 7.2. The wing has the planform parameter values

$$A = 8,\ \Lambda_{1/4} = 25° \text{ and } \lambda = 0.4,$$

and a constant streamwise section across the span, NACA 63_1-212, which is the same as that used in Example 1.

The flap has the same streamwise geometrical parameters as those used in Example 1 and extends from the wing centre-line to 60% of the wing semi-span. The location of the flap hinge-line is a constant proportion (75%) of the local wing chord. Note that this example is for the same planform as that in the example in Item No. 97011, in which the calculation of the required planform parameters and of a_1 is detailed.

The sweep angles $\Lambda_0 = 27.5°$ and $\Lambda_1 = 17°$, the planform parameter $A\tan\Lambda_0 = 4.16$, the Mach number and the Reynolds number, all lie within the ranges shown on Table 5.2.
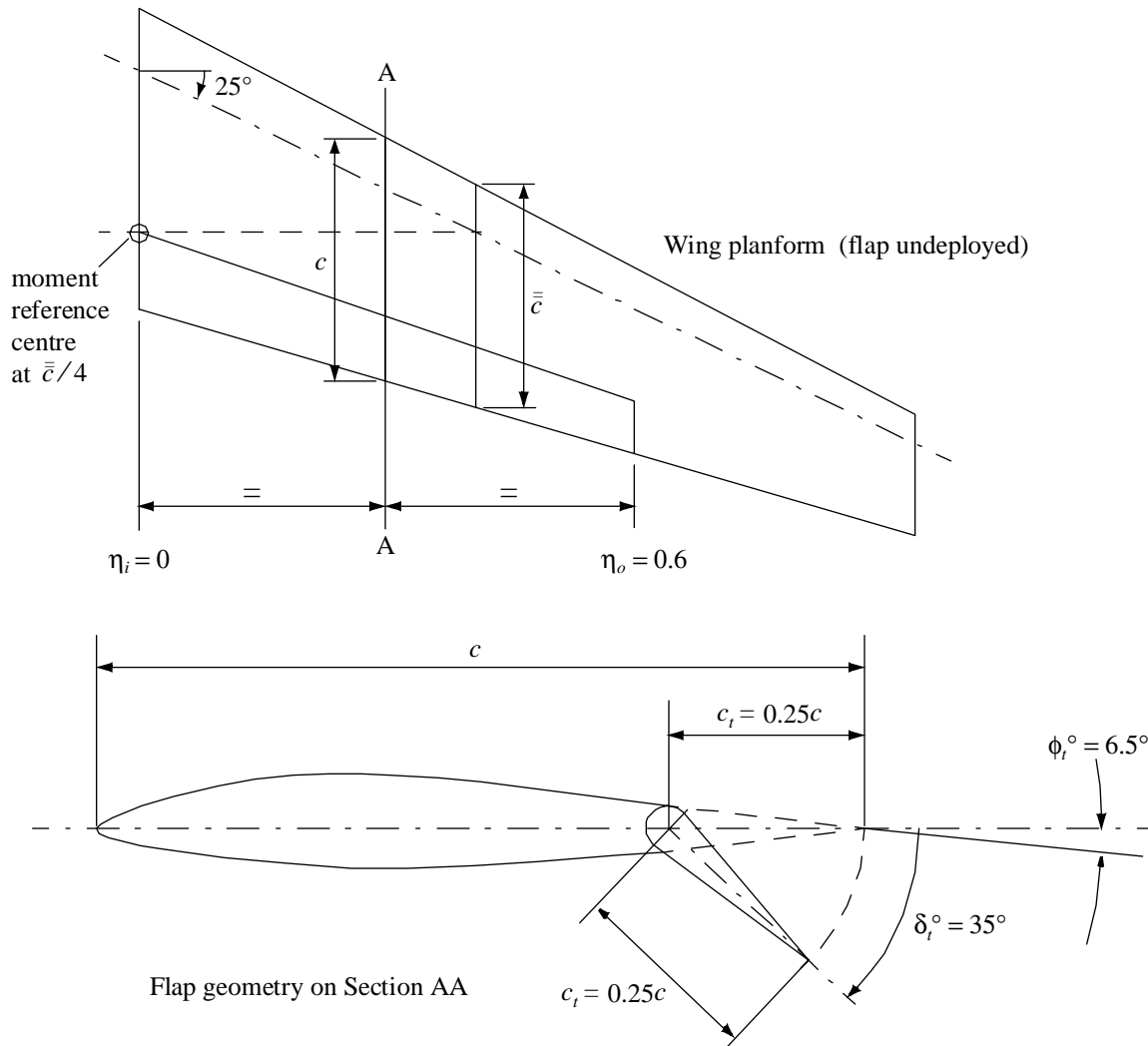
Sketch 7.2   Flap geometry on Section AA

(1)   **Determine ΔC_{L0t}**

Note that although this example is for the same section and flap geometry as for Example 1, the efficiency factor J_p for an aerofoil is replaced by J_{p0} for the section on a wing. The required value for a_t remains the same (0.0668) as for the aerofoil of Example 1.

From Figure 3, with $\delta_t° = 35°$ and $\phi_t° = 6.5°$ so that $\delta_t° + \phi_t° = 41.5°$,

$$J_{p0} \;=\; 0.580 \,.$$

From Equation (3.7)

$$\begin{aligned}
\Delta C_{L0t} \;&=\; J_{p0} a_t \delta_t° \\
&=\; 0.580 \times 0.0668 \times 35 \\
&=\; 1.356 \,.
\end{aligned}$$

(2) **Determine $\Delta C_{mtw\alpha 0}$**

From Equation (3.6)

$$\Delta C_{mtw\alpha 0} = -K_f (K_o - K_i)\Delta C_{L0t}h_2 + K_{f\Lambda}(K_{\Lambda o} - K_{\Lambda i})(A/2)\Delta C_{L0t}\tan \Lambda_{1/4}$$

in which h_2 has the same value (0.1833) as in Example 1.

From Figure 4 for $\eta_i = 0$ and $\lambda = 0.4$

$$K_i = 0$$

and for $\eta_o = 0.6$

$$K_o = 0.80 .$$

From Figure 5 for $\eta_i = 0$ and $\lambda = 0.4$

$$K_{\Lambda i} = 0$$

and for $\eta_o = 0.6$

$$K_{\Lambda o} = 0.0498 .$$

The flap type correlation factor K_f is given by Equation (3.8) as

$$K_f = (a_1/2\pi)^{0.46} .$$

With $A\tan\Lambda_{1/2} = 3.302$ and $\beta A = (1-0.2^2)^{1/2} \times 8 = 7.84$, a cross-plot in λ from Figures 1a to 1e of Item No. 70011, for $\lambda = 0.4$ gives
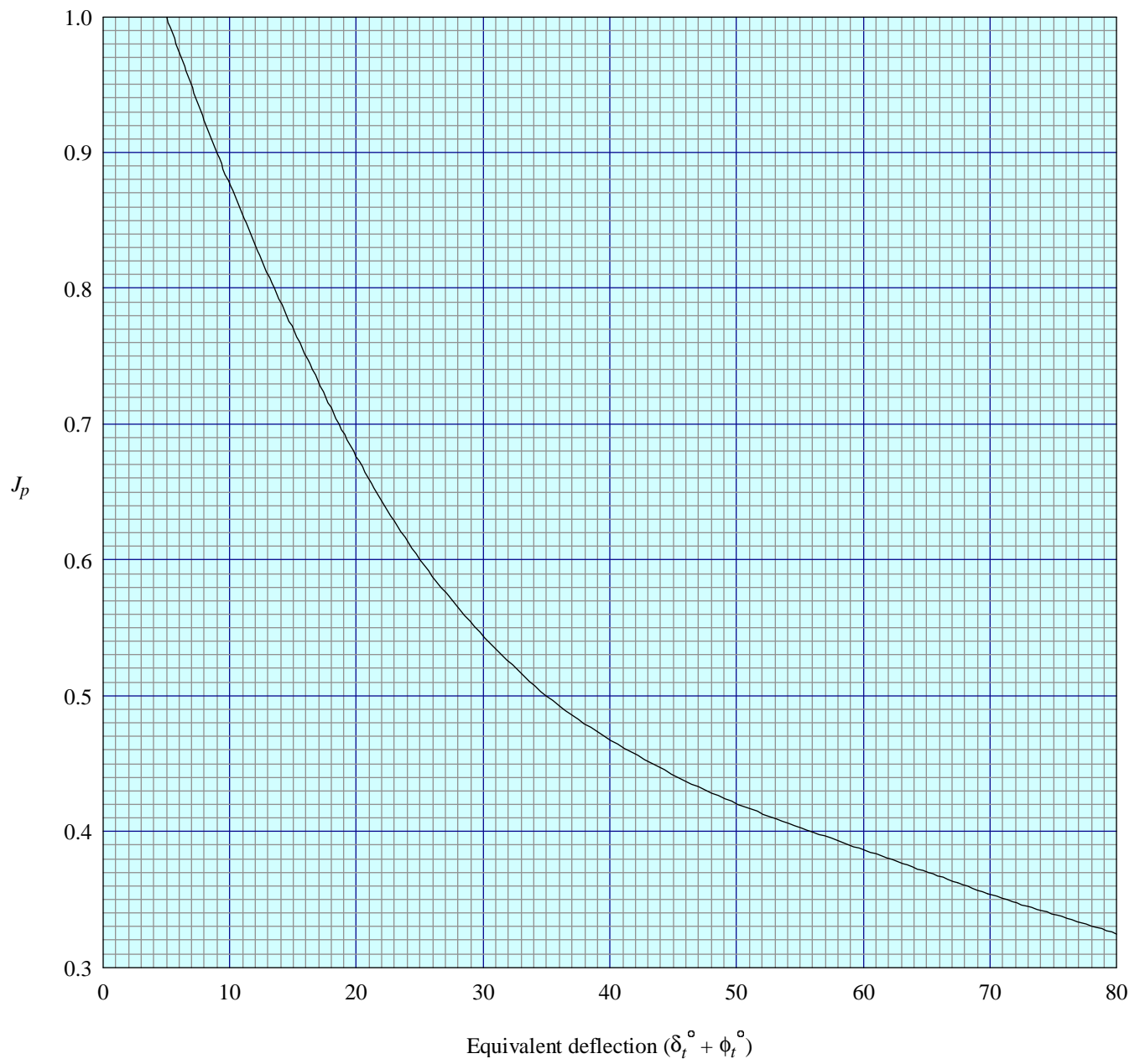
$$a_1 = 4.57 \text{ rad}^{-1} .$$

Thus $\quad K_f = (4.57/(2 \times 3.142))^{0.46}$

$$= 0.8637 .$$

The flap type correlation factor $K_{f\Lambda}$ is given by Equation (3.9) as

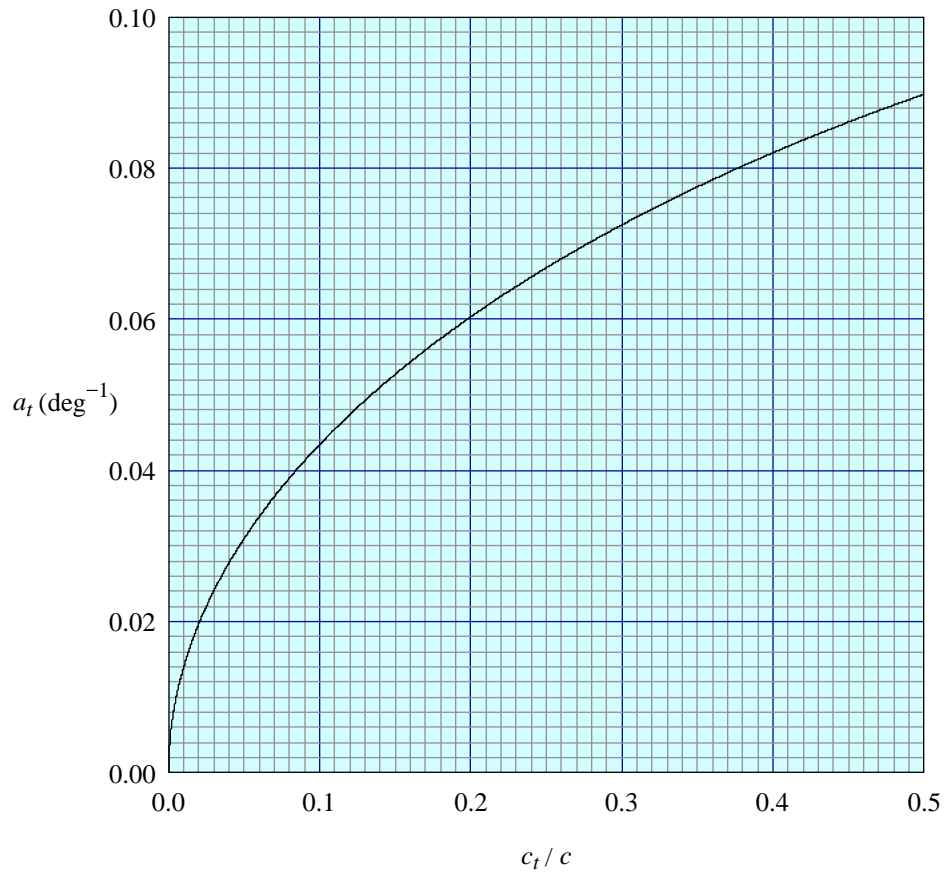$$K_{f\Lambda} = \cos \Lambda_{1/4}$$
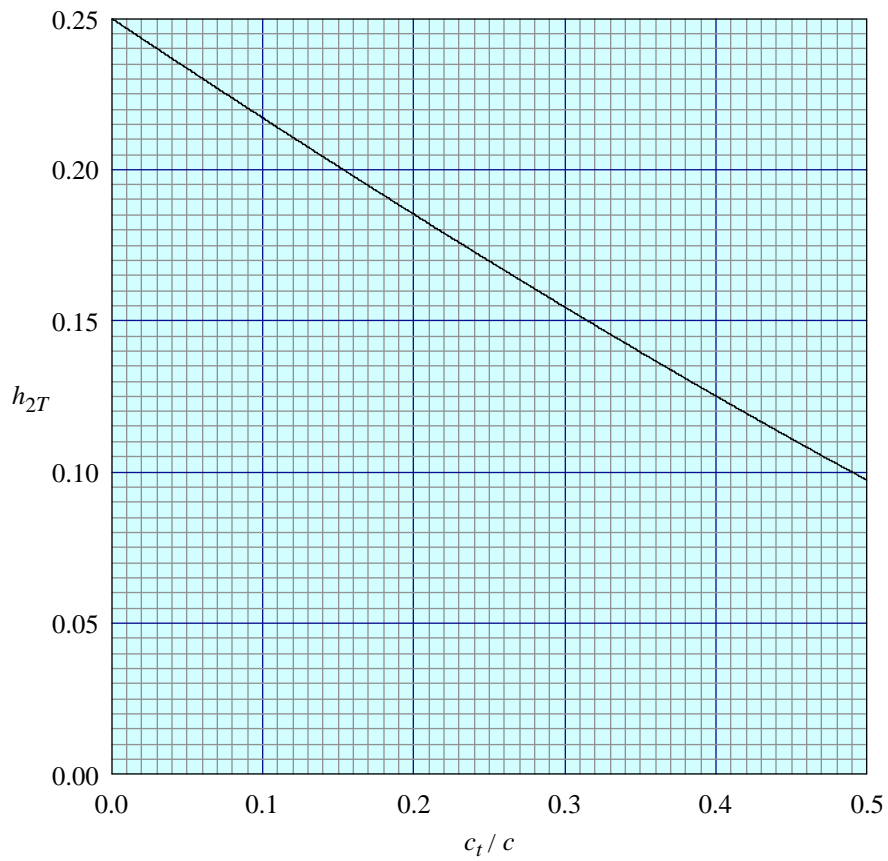$$= \cos 25^\circ$$
$$= 0.9063 .$$

Therefore

$$
\begin{aligned}
\Delta C_{mtw\alpha 0} &= -0.8637 \times (0.80 - 0.0) \times 1.356 \times 0.1833 \\
&\quad + 0.9063 \times (0.0498 - 0.0) \times 8/2 \times 1.356 \times \tan 25° \\
&= -0.2147 \times 0.8 + 0.9063 \times 0.0498 \times 4 \times 1.356 \times 0.4663 \\
&= -0.1718 + 0.1142 \\
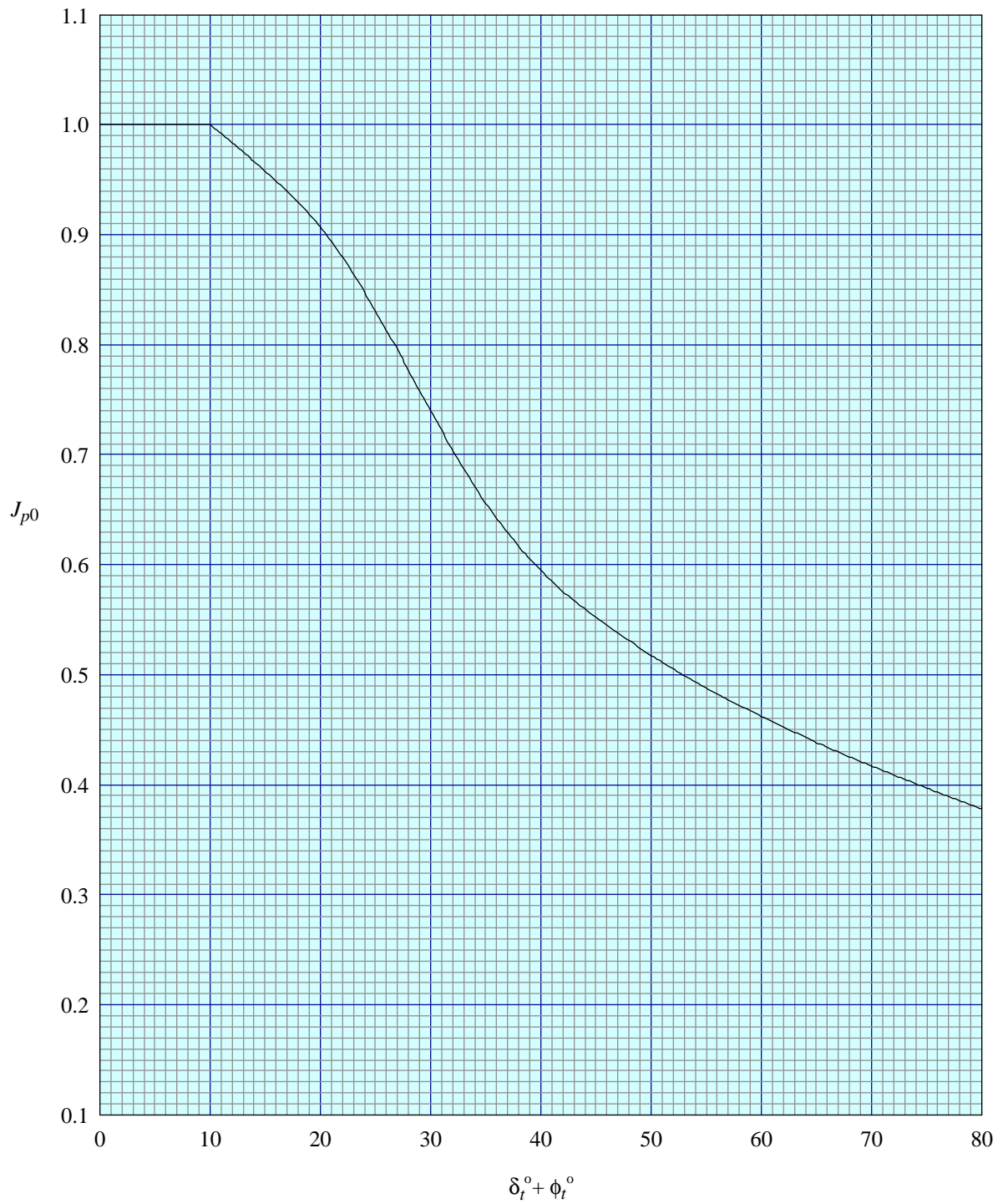&= -0.0576 \\
&\approx -\mathbf{0.058}.
\end{aligned}
$$

FIGURE 1 EFFICIENCY FACTOR J_p FOR PLAIN FLAP ON AN AEROFOIL

a_t (deg^{-1})

c_t / c

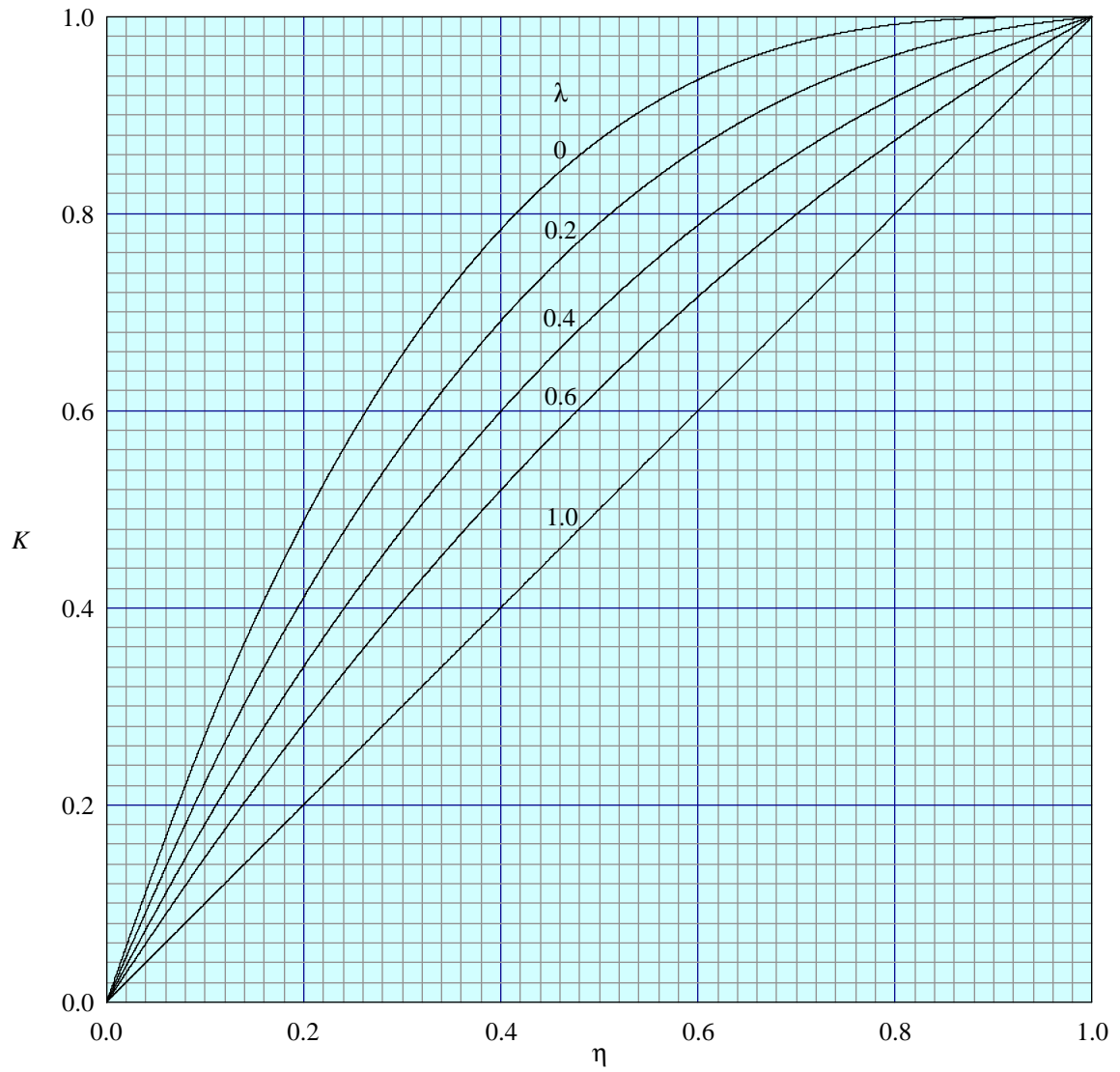FIGURE 2a VARIATION OF a_t WITH c_t/c

h_{2T}

c_t / c

FIGURE 2b VARIATION OF h_{2T} WITH c_t/c

FIGURE 3 EFFICIENCY FACTOR J_{p0} FOR PLAIN FLAP ON A WING

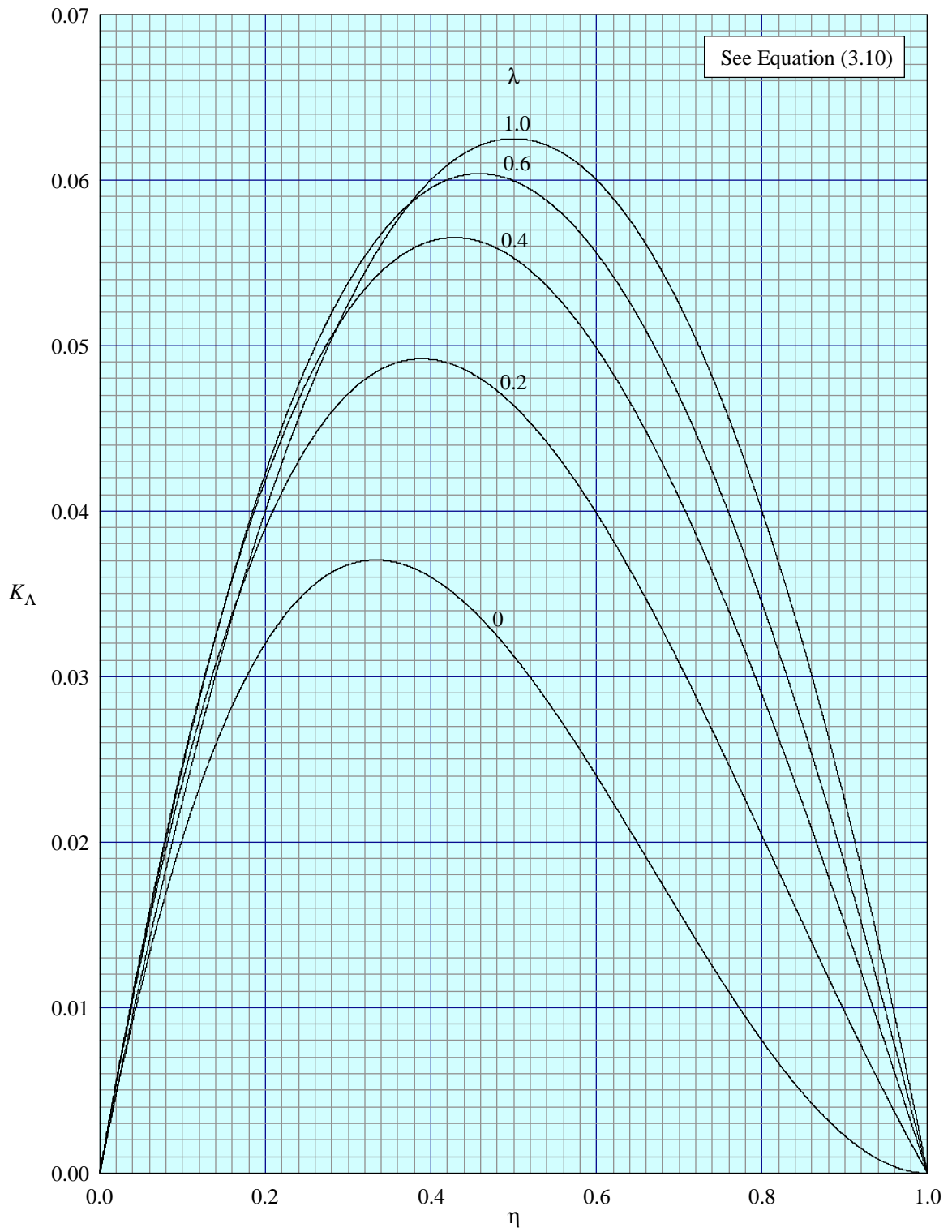**FIGURE 4 PART-SPAN FACTOR *K* FOR PLAIN FLAPS**

FIGURE 5 PART-SPAN FACTOR K_Λ FOR PLAIN FLAPS

THE PREPARATION OF THIS DATA ITEM

The work on this particular Data Item, which supersedes, in part, Item Nos Aero F.08.01.01 and 02 was monitored and guided by the Aerodynamics Committee, which first met in 1942 and now has the following membership:

Chairman

Mr H.C. Garner   –   Independent

Members

Dr M.Z. Bouter[*]	–	Raytheon Aircraft Co., Wichita, Kansas, USA
Mr P.D. Chappell	–	Independent
Dr P.C. Dexter	–	British Aerospace plc, Sowerby Research Centre, Bristol
Mr J.R.J. Dovey	–	Independent
Dr K.P. Garry	–	Cranfield University
Mr D.H. Graham[*]	–	Northrop Grumman Corp., Pico Rivera, Calif., USA
Mr M.J. Green	–	Independent
Dr H.P. Horton	–	Queen Mary and Westfield College, University of London
Dr D.W. Hurst	–	University of Glasgow
Mr M. Jager[*]	–	Boeing, Long Beach, Calif., USA
Mr K. Karling[*]	–	Saab-Scania AB, Linköping, Sweden
Dr E.H. Kitchen	–	Rolls Royce plc, Derby
Miss M. Maina	–	Aircraft Research Association
Mr M. Maurel	–	Aérospatiale, Toulouse, France
Mr C.M. Newbold	–	DERA, Farnborough
Mr J.B. Newton	–	British Aerospace Defence Ltd, Warton
Mr M.J. Pow	–	British Aerospace Airbus Ltd, Filton
Mr R. Sanderson	–	Daimler-Benz Aerospace Airbus, GmbH, Bremen, Germany
Mr J. Tweedie	–	Short Brothers plc, Belfast
Mr A.J. Wells	–	Avro International Aerospace, Woodford

[*]   Corresponding Member.

The technical work involved in the assessment of the available information and the development and subsequent construction of the Data Item method was carried out under contract to ESDU by Mr J.R.J. Dovey.